A New 82-kD Barbed End-capping Protein (Radixin) Localized in the Cell-to-Cell Adherens Junction: Purification and Characterization

Sachiko Tsukita, Yohki Hieda, and Shoichiro Tsukita

Department of Ultrastructural Research, The Tokyo Metropolitan Institute of Medical Science, Bunkyo-ku, Tokyo 113, Japan

Abstract. An 82-kD protein has been purified from the undercoat of the adherens junction isolated from the rat liver. The purification scheme includes low salt extraction followed by DEAE-cellulose ion exchange, DNase I-actin affinity, and carboxyl methyl-cellulose ion exchange chromatographies. The purified 82-kD protein was essentially free of contaminants as judged by SDS-PAGE combined with silver staining. The substoichiometric 82-kD protein largely inhibited the actin filament assembly; when the molar ratio of the 82-kD protein to G-actin was 1:1,000, the viscosity was reduced to 28% of the control value. Direct electron microscopic studies revealed that the 82-kD protein selectively inhibited monomer addition at the barbed ends of actin filaments. By use of the antibody raised against the 82-kD protein, this protein was shown by immunofluorescence microscopy to be localized at the cell-to-cell adherens junction in various types of cells. In contrast, the 82-kD protein was not concentrated at the cell-to-substrate adherens junctions (focal contacts). These findings have led us to conclude that the 82-kD protein is a barbed end-capping protein which is associated with the undercoat of the cell-to-cell adherens junction. Hence, we have tentatively designated the 82-kD protein as radixin (from the Latin word radix meaning root).

ADHERENS junctions are defined as one of the typical cell contacts in which actin filaments are associated with the plasma membrane through its well-developed undercoat (9, 12, 20, 38). To understand how the association between membranes and actin filaments is regulated, special interest has been focused on the molecular organization of the undercoat of adherens junctions. This junction was subclassified into two types: cell-to-cell and cell-to-substrate (16). Intensive studies, mainly by the use of immunological methods, have revealed that some unique proteins are localized in the undercoat of adherens junctions. For example, vinculin (12, 14–16), α-actinin (12, 14, 15, 25), $pp60^{src}$ (36), and plakoglobin (6, 10) are localized in the cell-to-cell adherens junction; and vinculin (11, 12, 14–16), α-actinin (12, 14, 15), $pp60^{src}$ (36), and talin (4) are localized in the cell-to-substrate adherens junction. However, our knowledge of the molecular organization of the undercoat is still fragmentary, partly because the biochemical enrichment procedure for this junction has not been available thus far.

Recently, we have succeeded in developing a new isolation procedure for the cell-to-cell adherens junction using rat liver, and in identifying 10 polypeptides including vinculin, α-actinin, and actin as major constituents of its undercoat (41). Our next step is to analyze the chemical nature of each constituent. Considering that actin filaments are associated with plasma membranes through the undercoat, it appears to be reasonable to search for the actin-binding proteins among the major constituents of the undercoat. Our preliminary experiments using DNase I affinity chromatography have revealed that the polypeptide with the molecular mass of 82 kD shows a rather strong G-actin-binding ability. Therefore, as a first step to systematically analyze the chemical properties of each constituent of the undercoat of adherens junctions, we have chosen to focus on this 82-kD protein. In this paper, we describe the purification of the 82-kD protein, its biochemical properties in vitro, and its localization in vivo. The results obtained have indicated that this 82-kD protein is the barbed end-capping protein localized in the cell-to-cell adherens junction.

Yohki Hieda's present address is Department of Molecular Biology, Faculty of Science, Nagoya University, Chikusa-ku, Nagoya 464, Japan.

Materials and Methods

Purification of the 82-kD Protein

All procedures were performed at 4°C. The 82-kD protein was purified from the low salt extract of the adherens junction fraction. The adherens junction was prepared from rat liver by the combination of homogenization, sucrose density-gradient centrifugation, and Nonidet treatment described previously (41). The first low salt extract (30 ml of 0.2 mg/ml) was obtained by dialysis of the adherens junction fraction from 12 rat livers against the extraction solution (1 mM EGTA, 0.5 mM PMSF, 1 μg/ml leupeptin, 2 mM Tris-HCl, pH 9.2), followed by centrifugation at 100,000 *g* for 60 min. The

pellet was resuspended in 20 ml of the extraction solution and dialyzed again against the same solution. The second extract (0.1 mg/ml) was obtained by centrifugation at 100,000 *g* for 60 min.

Preswollen DEAE-cellulose was packed into a column (1 × 5 cm) and equilibrated with buffer A composed of 10 mM Hepes, 1 mM EGTA, 0.1 mM DTT, 1 μg/ml leupeptin, 1 mM PMSF (pH 7.5). The first and second low salt extracts were sequentially applied onto the DEAE-cellulose column. The column was washed with 100 ml of buffer A before eluting with 60 mM KCl/buffer A (pH 7.5), 150 mM KCl/buffer A (pH 7.5), and 300 mM KCl/buffer A (pH 7.5), sequentially. When fractions were assayed for the 82-kD protein by SDS-PAGE, the 82-kD protein was enriched in the 60 mM KCl/buffer A elute. The 60-mM KCl elute was then mixed with an equal volume of buffer B (2 mM Hepes, 0.2 mM ATP, 0.2 mM DTT, 1 mM *p*-Toluenesulfonyl-L-arginine methyl ester hydrochloride [Tame], 1 mM PMSF, 1 μg/ml leupeptin, pH 7.5) and loaded on the DNase I-actin affinity column (1 × 1.5 cm). This column was prepared by mixing gel-filtrated G-actin (5 mg) with DNase I-coupled Affi-Gel 10 (see references 19, 27), followed by thoroughly washing with buffer B, 400 mM KCl/buffer B, and buffer B, sequentially. After applying the sample, the DNase I-actin affinity column was washed with 30 mM KCl/buffer C (the 1:1 mixture of buffer A and buffer B, pH 7.5) and then the 82-kD protein was eluted from the column with 160 mM KCl/buffer C (pH 7.5). In a final step, the fraction enriched in the 82-kD protein was passed through carboxyl methyl (CM)[1]-cellulose column (equilibrated with 160 mM KCl/buffer C, pH 7.5), and the purified 82-kD protein was recovered in the fractions that were slightly retarded from the void volume fractions.

Preparation of G-Actin

Rabbit skeletal muscle G-actin was prepared by the method of Spudich and Watt (37) and further purified by gel filtration on a Sephadex G-100 column equilibrated with buffer G (2 mM Tris, 0.2 mM ATP, 0.5 mM DTT, pH 7.5) (19, 35).

Assay for the Effects of 82-kD Protein on Actin Polymerization

Falling Ball Viscometry Assay. 100 μl of the purified 82-kD protein (0–0.5 μg/ml) in 160 mM KCl/buffer C was mixed with 210 μl of buffer G and warmed for 5 min at 25°C. Actin polymerization was induced by addition of 90 μl of gel-filtrated G-actin which was prewarmed for 5 min at 25°C. The mixture was immediately drawn into 10 capillary tubes (50-μl micropipettes; Clay-Adams, Inc., Parsippany, NJ). A stainless steel ball of 0.5 mm diam was inserted into each micropipette. The time for the ball to fall a distance of 1 cm at a declination of angle θ ($\tan\theta = 1/3$) was recorded at 25°C (29, 30). Annealing rates were measured as the rate of viscosity recovery after fragmenting a steady-state mixture of actin filaments into short segments by pipetting. After pipetting, 100 μl of the actin filament solution (3 mM $MgCl_2$, 0.5 mg/ml) was added into the mixture of the 82-kD protein solution (100 μl of 160 mM KCl/buffer C; 0 or 0.25 μg/ml) and buffer G (100 μl). The final mixture was immediately drawn into the micropipettes. The recovery of viscosity was estimated by recording the time for the stainless steel ball to roll a distance of 1 cm of the micropipettes.

Electron Microscopy. The effect of the 82-kD protein on the actin polymerization was examined by using the acrosomal processes to nucleate filament assembly or by using the polystyrene beads. *Limulus* sperm acrosomal processes were prepared according to the procedure of Tilney (39), and stored in 50% glycerin, 15 mM Tris-HCl, 1.5 mM $MgCl_2$, 50 μM EDTA (pH 7.5) at −20°C (2, 3, 26). 50 μl of the acrosomal processes was mixed with 200 μl of distilled water at 4°C and fragmented into short pieces by sonication (10 W × 10 s). After centrifugation at 15,000 *g* for 10 min, the lowest one-third of the solution was used as the final acrosomal process preparation. For the actin polymerization experiment, 35 μl of the 82-kD protein (0 or 1 μg/ml) in 160 mM KCl/buffer C was mixed with 70 μl of acrosomal process solution and 70 μl of distilled water, and preincubated at 4°C for 15 min. Actin polymerization was initiated by addition of 50 μl of gel-filtrated G-actin (0.5 mg/ml) in buffer G. After polymerization of actin in the presence or absence of the 82-kD protein at room temperature for 40 s or 10 min, the samples were mounted on the collodion-coated copper grids. The sample was negatively stained with 4% aqueous uranyl acetate, and examined in the JEOL 1200-EX electron microscope operated at 100 kV. Some samples were incubated on the grid with some drops of heavy meromyosin (HMM) solution (2 mg/ml in 30 mM KCl/buffer A) at room temperature for 1 min before negative staining.

For the polymerization experiment of G-actin on polystyrene beads (21), 10 μl of the 82-kD protein (1 μg/ml) in 160 mM KCl/buffer C was preincubated at 4°C for 10 min with 30 μl of buffer G containing polystyrene beads (PSI-68; Rhone-Poulenc, Ltd., France). 5 μl of gel-filtrated G-actin (0.5 mg/ml) was added and incubated at room temperature for 10 min. The samples were negatively stained and examined in the electron microscope.

Immunological Methods

Anti-82-kD Protein Antibody. Antisera to the 82-kD protein purified by SDS-PAGE were elicited in rabbits, and IgG was purified from the sera, according to the methods described previously (41). Antivinculin antibody was also obtained in the same procedure (41). Mouse monoclonal antibody directed against plakoglobin was purchased from Progen Biotechnics (Heidelberg, FRG). Antidesmoplakin polyclonal antibody raised in guinea pigs was a generous gift from Dr. A. Kusumi (University of Tokyo, Tokyo, Japan).

Immunoblotting and Indirect Immunofluorescence Microscopy. For immune blotting, the samples were electroblotted onto nitrocellulose membranes after SDS-PAGE (42). The strips of the nitrocellulose membranes were incubated with first antibody and then treated with the second horseradish peroxidase-labeled antibody (Bio-Rad Laboratories, Richmond, CA). The peroxidase was detected by the reaction using diaminobenzidine in the presence of Ni and Co ions (8). For indirect immunofluorescence microscopy of cultured cells, Madin-Darby bovine kidney (MDBK) epithelial cells and primary rat epidermal keratinocytes (prepared as described previously [17, 33]) were fixed with 1% formaldehyde in PBS for 15 min at room temperature, treated with 0.2% Triton X-100 in PBS in 15 min, and washed three times with PBS. After being soaked in PBS/1% BSA for 10 min, the cells were treated with first antibody diluted with PBS/1% BSA. They were washed with PBS/1% BSA and incubated with second antibody coupled with FITC or rhodamine for 30 min. The sample was washed with PBS three times and examined with an Olympus Corp. (New Hyde Park, NY) Vanox-S microscope. For indirect immunofluorescence microscopy of frozen sections, samples were frozen by liquid N_2 and ~10-μm-thick frozen sections were fixed in 95% ethanol at −20°C for 30 min and in 100% acetone at room temperature for 5 min (40).

Immunoelectron Microscopy. The fraction rich in bile canaliculi was obtained as described in the preceding paper (41). The bile canaliculi were suspended in 1% BSA/TBS (150 mM NaCl, 10 mM Tris, pH 7.5) containing 1/50 vol of anti-82-kD protein IgG or antivinculin IgG. After a 90-min incubation at room temperature, samples were washed three times by centrifugation at 10,000 *g* for 10 min in TBS/1% BSA. The final pellet was incubated with goat anti-rabbit IgG coupled to 10-nm gold (GAR G-10; Janssen Life Sciences Products, Piscataway, NJ) which was diluted tenfold with TBS/1% BSA. The samples were washed twice with TBS/1% BSA and once with PBS (150 mM NaCl, 10 mM $NaPO_4$, pH 7.4) by centrifugation at 10,000 *g* for 10 min. The pellets obtained were fixed in 0.1% tannic acid, 2.5% glutaraldehyde, 0.1 M sodium cacodylate, pH 7.4, fixed afterward in 1% OsO_4, 0.1 M sodium cacodylate (pH 7.4), washed in distilled water, stained en bloc with 0.5% aqueous uranyl acetate, and embedded in Epon 812. Sections were stained doubly with uranyl acetate and lead citrate before being viewed in a JEOL 1200-EX electron microscope.

SDS-PAGE

SDS-PAGE was based on the discontinuous Tris-glycine system of Laemmli (24). The stain Coomassie brilliant blue R-250 or the silver stain (Wako silver staining kit) was used.

Results

Purification of 82-kD Protein from Adherens Junction-rich Fraction

A number of analyses using DNase I affinity column chromatograpy have shown that four types of actin-modulating proteins are trapped by this column through the specific affinity with G-actin: profilin-type (5), depactin-type (27), cofilin-type (32), and barbed end-capping protein-type (7, 18, 19, 23, 28, 43). Among them, cofilin and the barbed end-capping protein types can bind to F-actin as well as to G-ac-

1. *Abbreviations used in this paper*: CM, carboxyl methyl; HMM, heavy meromyosin; MDBK, Madin-Darby bovine kidney.

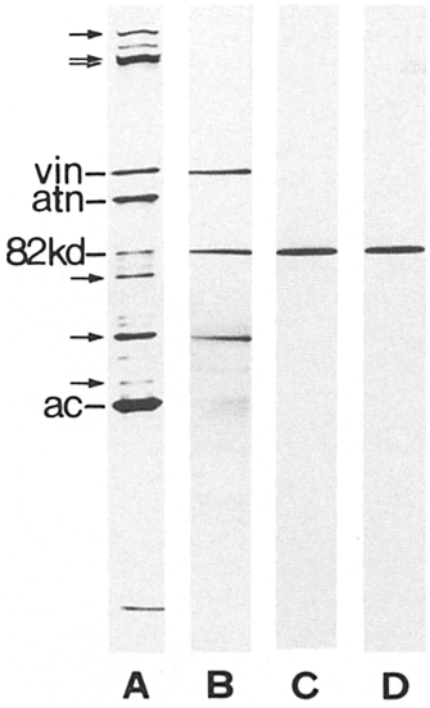

Figure 1. SDS–polyacrylamide gels showing the protein profiles during the purification of the 82-kD protein by silver staining. (Lane *A*) Low ionic strength extract of the adherens junction. The extract shows the typical electrophoretic pattern of the major constituents including vinculin (*vin*),α-actinin (*atn*), the 82-kD protein (*82kd*), actin (*ac*), and several other proteins (*arrows*) (see reference 41). (Lane *B*) DEAE–cellulose column elute (60 mM KCl) enriched in vinculin, 82-kD protein, and 55-kD protein. (Lane *C*) The 82-kD protein eluted from DNase I–actin affinity column. (Lane *D*) The 82-kD protein purified by the CM–cellulose column chromatography.

tin. When the low salt extract of adherens junction was applied to the DNase I affinity column, the polypeptide with the molecular mass of 82 kD was the main component that was trapped and released by washing the column with 600 mM KCl solution (data not shown); the 82-kD protein comprised ~80% of the trapped proteins as estimated on the SDS–polyacrylamide gels. Considering that the isolated adherens junction fraction contains F-actin, but not G-actin, it is reasonable to assume that this 82-kD protein may be categorized into the cofilin or barbed end–capping protein type. To determine to which type this 82-kD protein belongs, we have attempted to purify this 82-kD protein from the adherens junction–rich fraction.

The purification scheme of the 82-kD protein includes low ionic strength extraction of the adherens junction fraction, and the DEAE–cellulose ion exchange, DNase I–actin affinity, and CM–cellulose ion exchange chromatographies, as described in detail in Materials and Methods. The protein compositions at each step of the purification are displayed on SDS–polyacrylamide gels in Fig. 1. Vinculin and the 82-kD protein were copurified by DEAE–cellulose chromatography, and separated on a DNase I–actin affinity column. The resultant preparation of the 82-kD protein was essentially free of contaminants as judged by SDS-PAGE combined with silver staining. Upon storage, some bands on SDS–polyacrylamide gels with molecular masses of 80 kD and 30–35 kD often were seen to appear. The increase of these bands with time suggested that they were probably proteolytic degradation products. The amount of the 82-kD protein in the adherens junction was rather small, and only 1 μg of the 82-kD protein was purified from 8 mg protein of low salt extract of the adherens junction fraction (which was prepared from 12 rats, 150 g of liver).

Interaction of the 82-kD Protein with Actin

Falling Ball Viscometry Assay. The effects of 82-kD protein on the initial rate of actin polymerization and the final viscosity level of the polymerized actin were examined by the falling ball viscometry assay. The initial rate of viscosity increase was accelerated by the substoichiometric concentrations of the 82-kD protein (Fig. 2 *A*). The final steady-state viscosity was reduced prominently with substoichiometric concentrations of the 82-kD protein; when the molar ratio of the 82-kD protein to actin monomer was 1:3,000, 1:2,000, and 1:1,000, the steady-state viscosities were reduced to 78, 60, and 28%, respectively, of the control viscosity (obtained by the G-actin polymerization in the absence of 82-kD protein). These effects of 82-kD protein on actin polymerization were not influenced by Ca^{2+} in the polymerization solution. Next, we examined the effects of the 82-kD protein on annealing of actin filaments; actin filaments at steady state were passed through a micropipette several times in the presence or absence of 82-kD protein, and then the recovery of viscosity was monitored using falling ball viscometry assay. In the absence of 82-kD protein, the viscosity returned to the original level within 60 min. However, in the presence of substoichiometric concentration of 82-kD protein (the molar ratio of the 82-kD protein to actin is 1:2,000), the recovery of viscosity was inhibited to 60% (data not shown).

When these findings are taken together, it is reasonable to speculate that the 82-kD protein is a kind of capping protein. To evaluate this speculation, and, if so, to determine the end to which the 82-kD protein binds, we have examined the effects of 82-kD protein on the actin filament growth on barbed and pointed ends of actin filaments by direct electron microscopic observations.

Electron Microscopy. By the use of short segments of actin bundles of isolated *Limulus* acrosomal processes (referred to here as acrosomal processes) as nuclei of actin polymerization, it is possible to directly examine the nucleated polymerization of G-actin at both ends of actin filaments of acrosomal processes by negative-staining electron microscopy (2, 3, 26, 35). Using this method, we examined the nucleated polymerization of actin filaments in the presence or absence of the 82-kD protein (Figs. 2–4).

When the acrosomal processes were incubated with G-actin for a short time period (40 s) in the absence of the 82-kD protein, actin was polymerized into 0.5-μm-long filaments at only one end of 81% of the processes (Fig. 2, *B–D*). As judged by the recent kinetic studies (30, 35), these active ends can be regarded as the barbed ends. In contrast, when the processes were preincubated with the 82-kD protein (1 μg/ml) followed by incubation with G-actin in the presence of 82-kD protein (the molar ratio of 82-kD protein to G-actin was nearly 1:1,400), no actin filaments were associated with 75% of processes (Fig. 2 *E*). These results favored the idea

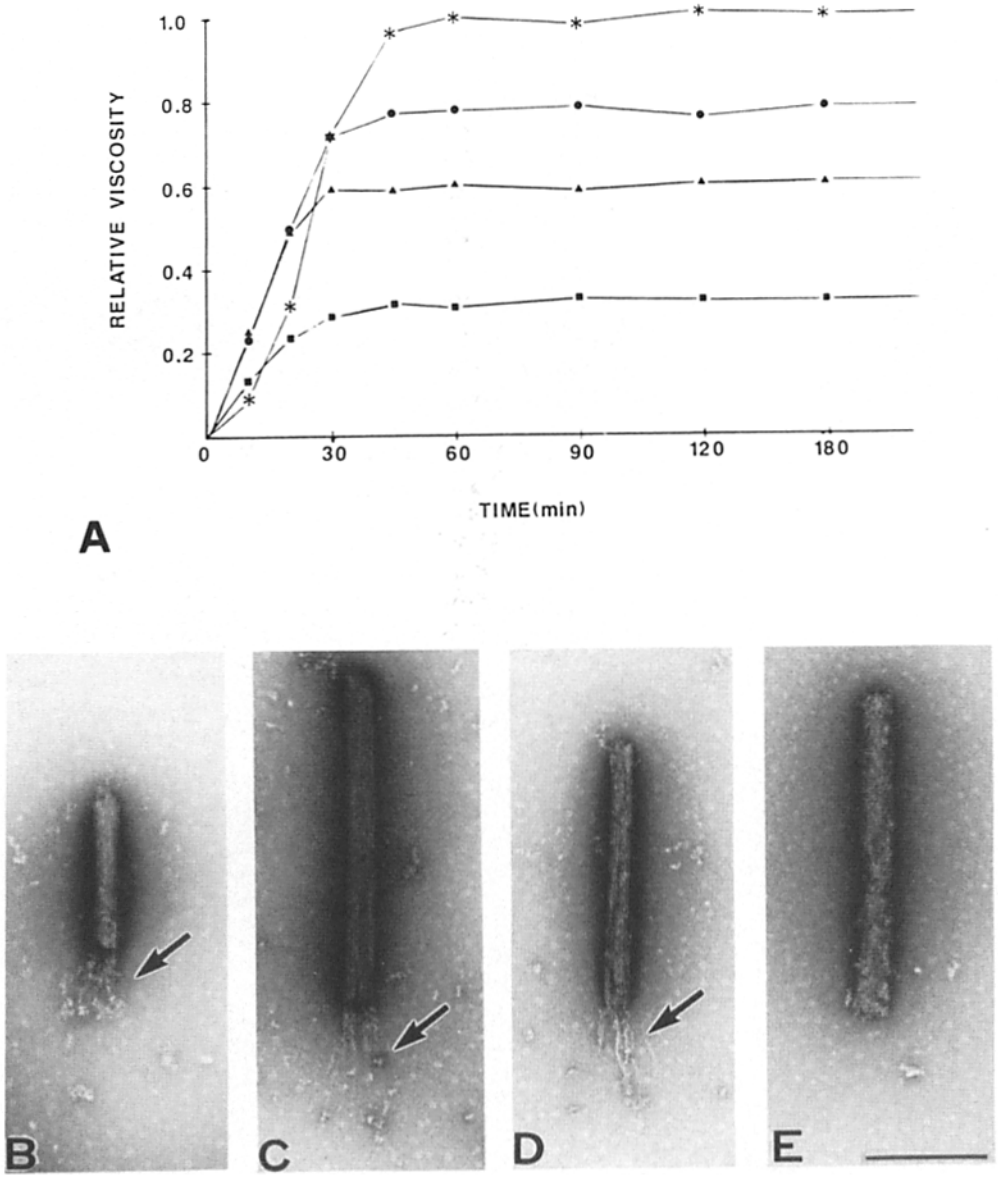

Figure 2. (*A*) Falling ball viscometry in the absence (*) or presence of increasing concentrations of the 82-kD protein at the molar ratio of 1:3,000 (●), 1:2,000 (▲), and 1:1,000 (■) of 82-kD protein to actin. (*B–E*) Negative staining electron micrographs showing the effect of the 82-kD protein on the actin polymerization by the use of acrosomal processes. (*B–D*) When the acrosomal processes are incubated with G-actin in the absence of the 82-kD protein for a short time period (40 s), short actin filaments are associated with only one end of 81% of the acrosomal processes (*arrows*). (*E*) In contrast, no filament growth is observed on 75% of the processes when the processes are preincubated with the 82-kD protein followed by the incubation with G-actin in the presence of the 82-kD protein. Bar, 0.5 μm.

that the 82-kD protein inhibited the barbed end growth of actin filaments. To further confirm this point, we took advantage of HMM decoration at the next step.

When the acrosomal processes were incubated with G-actin in the absence of 82-kD protein for a relatively long time period (10 min) to allow polymerization at both barbed and pointed ends, actin filaments elongated bidirectionally with a prominent bias of the elongation rate for the barbed end, as judged by HMM decoration (Fig. 3 *A*). In contrast, when the acrosomal processes were preincubated with the 82-kD protein (1 μg/ml) followed by incubation with G-actin in the presence of the 82-kD protein (the molar ratio of the 82-kD protein to G-actin is 1:1,400), the actin polymerization at barbed ends was largely inhibited, while the polymerization at pointed ends was not influenced (Fig. 3, *B* and *C*). The statistical results are shown in Fig. 4 *A*. Next, we examined the polarized polymerization of G-actin on the carboxyl-rich polystyrene beads in the presence or absence of 82-kD protein (Fig. 4, *B* and *C*). In the absence of the 82-kD protein as a control experiment, actin monomers were polymerized with 7:3 bias for the barbed ends. In contrast, when the beads were incubated with 82-kD protein and then with G-actin in the presence of 82-kD protein, the growing filaments were directed with 7:3 bias for the pointed ends. These results indicated that the pointed ends were much favored for polymerization in the presence of the 82-kD protein.

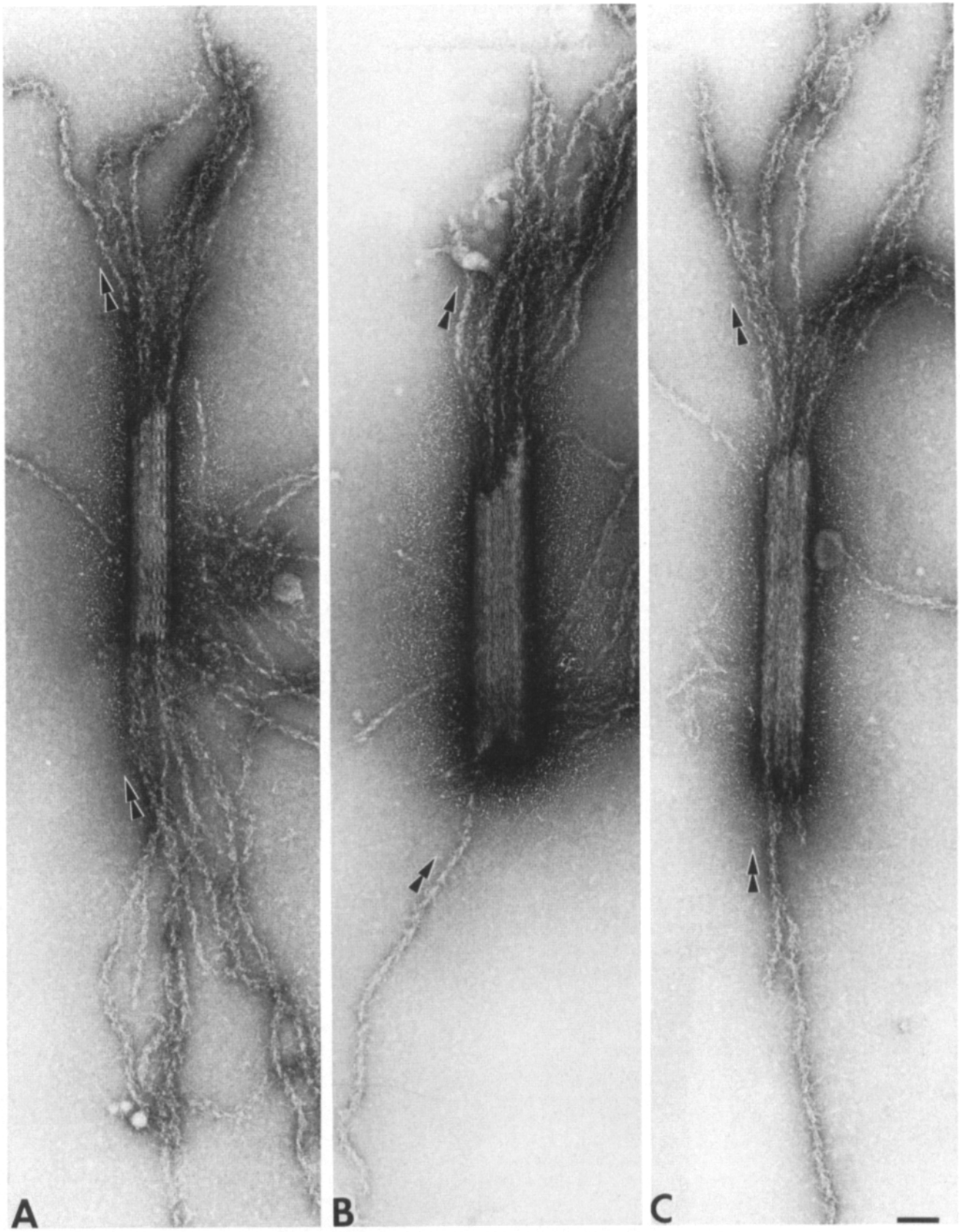

Figure 3. Negative-stained acrosomal processes after incubation with G-actin in the absence (*A*) or presence (*B* and *C*) of the 82-kD protein followed by HMM decoration. (*A*) Both barbed and pointed ends of the actin bundles of acrosomal processes nucleate for actin filament elongation. The directionality of growing actin filaments is shown by the HMM decoration method (*arrowheads*). (*B* and *C*) The 82-kD protein selectively inhibits the polymerization of actin filaments at the barbed ends of the actin bundles of acrosomal processes, while it does not influence the polymerization at the pointed ends. As a result, most actin filaments are directed with arrowheads of HMM pointing away from the acrosomal processes. Bar, 0.1 μm.

ACROSOMAL PROCESS NUCLEI

Conditions		Directionality 0–5 Filaments	>5 Filaments
CONTROL	Barbed Ends	12%	88%
	Pointed Ends	20%	80%
+RADIXIN	Barbed Ends	53%	47%
	Pointed Ends	18%	82%

A

BEADS NUCLEI

Conditions		Directionality
CONTROL	Barbed Ends	70%
	Pointed Ends	30%
+RADIXIN	Barbed Ends	33%
	Pointed Ends	67%

B

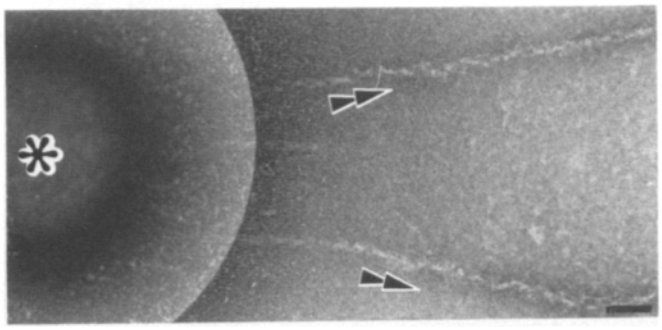

C

Figure 4. (*A* and *B*) Quantification of the effect of a substoichiometric amount of radixin (the 82-kD protein) on the polymerization of actin filaments at both barbed and pointed ends. 50 acrosomal processes were examined by negative-staining electron microscopy. The percentages given are derived from the number of actin filaments grown from the barbed or pointed ends of the nuclei (acrosomal processes in *A* or beads in *B*). Note that radixin (the 82-kD protein) dramatically inhibits the polymerization of actin at the barbed ends. (*C*) Negative-staining electron microscopy of the growing actin filaments from the beads (*asterisk*) in the presence of radixin. The polarity of the actin filaments are largely biased for the pointed ends (*arrowheads*), resulting in the filaments depicted with arrowheads of HMM pointing away from the bead. The portion around the bead is printed lighter to reveal the attachment of actin filaments. Bar, 0.1 μm.

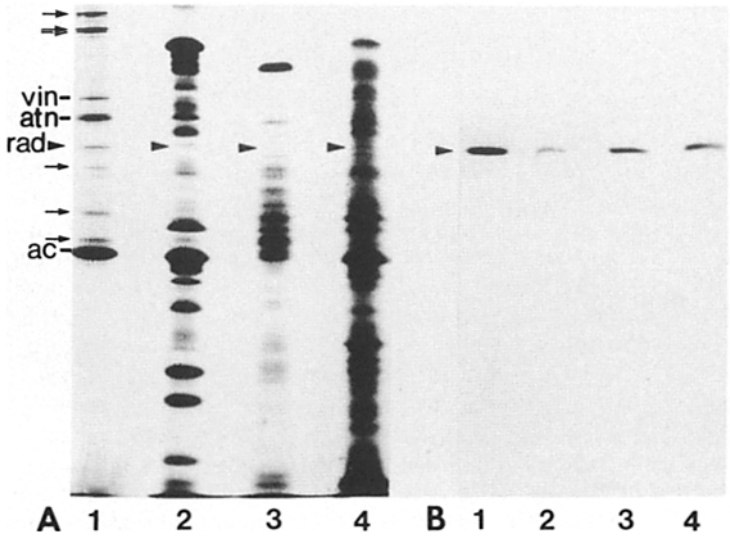

Figure 5. Antiradixin immunoblotting of rat tissues. Coomassie blue-stained gels (*A*) and the corresponding immunoblot profiles with the antiradixin antibody (*B*). (Lanes *1*) Extract of adherens junction which is mainly composed of vinculin (*vin*), α-actinin (*atn*), radixin (*rad*), actin (*ac*), and several other polypeptides (*arrows*). (Lanes *2*) Cardiac muscle; (lanes *3*) liver; (lanes *4*) small intestine. The immunoblot profiles show cross-reactivity of radixin (the 82-kD protein) in cardiac muscle, liver, and small intestine (*arrowheads*).

In summary, these results have led us to conclude that the 82-kD protein is a kind of a barbed end–capping protein. Accordingly, this protein is tentatively designated as "radixin" (from the Latin word radix meaning root) in this paper.

Immunochemical Characterization of Radixin by Immunoblot

Radixin was purified electrophoretically from the low salt extract of adherens junction, and antisera to this protein were raised in rabbits. IgG was purified from the serum using ammonium sulfate precipitation and DEAE-cellulose column chromatography. By the immunoblotting procedure, it became clear that this IgG specifically reacted with radixin in the adherens junction extract (Fig. 5) and with the purified radixin (data not shown). This antibody also recognized a single band of identical value (82 kD) in homogenate from all adherens junction–bearing cells studied, such as rat liver, heart, intestine, and MDBK cells (Fig. 5).

Localization of Radixin in Frozen Sections of Various Tissues

Since, by immunoblotting assays, radixin was detected in the adherens junction–bearing tissues such as rat liver, heart, and intestine, the localization of radixin was examined by immunofluorescence microscopy on frozen sections of these tissues. For comparison, the frozen sections were also stained by anti-rat vinculin antibody (41).

In the liver, both antiradixin and antivinculin antibodies stained the junctional complex region of the liver cells (Fig. 6). When frozen sections were stained for vinculin in cross section, a pair of dots on both sides of the bile canaliculi were observed, while in longitudinal section a pair of parallel lines running along the lateral cell surface were visible (Fig. 6 *C*). In the frozen sections immunofluorescently stained for radixin, similar staining patterns were obtained (Fig. 6 *A*). Close inspection, however, has revealed that the linear staining patterns differ in appearance between radixin and vinculin stainings; i.e., rough and smooth lines, respectively (Fig. 6, *B* and *D*). Furthermore, in the case of radixin distribution, the spotted staining was seen to be scattered in the cytoplasm, in addition to the linear staining. Similar staining was also observed in other types of cells (see Figs. 8 *B* and 9 *D*), but it remained to be clarified what this staining reflected. To confirm that these linear stainings correspond to the belt-like adherens junctions, an isolated bile canaliculi-enriched fraction was used to immunolocalize radixin and vinculin at the electron microscopic level (Fig. 6, *E* and *F*). Both antiradixin and antivinculin antibodies specifically labeled the cytoplasmic side of the adherens junctions. No labeling was detected on nonjunctional membranes. The distances between the antigens and membranes could not have been discussed in these preparations, partly because the undercoats of adherens junctions might be disorganized during treatments with antibodies and partly because antibodies might not easily reach the antigens which were embedded within the undercoat. In the intestinal epithelial cells, the antiradixin antibody strongly stained their terminal web (Fig. 7, *A* and *B*), similarly to the vinculin staining (data not shown, see reference 15). Taken together, it is safe to say that radixin is localized in the cell-to-cell adherens junction.

When frozen sections of rat cardiac muscle were examined by the immunofluorescence microscopy using both antivinculin and antiradixin antibodies, the staining patterns of these antibodies were distinct (Fig. 7, *C* and *D*). In both cases extensive labeling of the intercalated discs was observed, but only in the case of vinculin was the patchy labeling detected periodically along the lateral borders of the cells ("costamere" pattern) (34). These observations led us to speculate that, in contrast to vinculin, radixin was localized only in the cell-to-cell adherens junction, but not in the cell-to-substrate adherens junction. To confirm this speculation, the distribution of radixin was further examined in cultured cells.

Localization of Radixin in Cultured Cells

The distributions of vinculin and radixin were compared by double immunofluorescence microscopy in MDBK epithelial cells (Fig. 8, *A* and *B*). As shown previously (references 11–15), vinculin staining was found at both cell-to-cell and cell-to-substrate adherens junctions, although the staining of the cell-to-cell adherens junction was found on the focus plane above the substrate (Fig. 8 *A*). Radixin staining was localized specifically at the cell-to-cell adherens junction, while it did not appear to be associated with the cell-to-substrate junctions (Fig. 8 *B*). Careful observation has revealed again that the linear stainings at the cell-to-cell adherens junction were different in appearance between vinculin and radixin staining; i.e., smooth and rough, respectively. Radixin showed additional dotted stainings in the cytoplasm of MDBK cells, similar in situation to the liver cells in frozen sections (see Fig. 6 *A*). To clearly demonstrate the absence of radixin from the cell-to-substrate adherens junction, the rat fibroblasts (3Y1) were stained with antivinculin and antiradixin antibodies (Fig. 8, *C* and *D*). Intensive vinculin staining was detected at the cell-to-substrate adherens junctions (focal contacts) (Fig. 8 *C*), while these junctions were by no means labeled by antiradixin antibody (Fig. 8 *D*). Furthermore, we have examined the distribution of vinculin and radixin in rat keratinocytes cultured under low and normal calcium conditions (Fig. 9). Under the low calcium condition, the cell-to-cell adherens junctions were not formed; the cell-to-substrate junctions were clearly stained by antivinculin antibody (Fig. 9 *A*), but not by antiradixin antibody (Fig. 9 *B*). When the cells were cultured under normal calcium condition, the cell-to-cell adherens junctions were induced. These junctions were strongly stained with antiradixin as well as with antivinculin antibody (Fig. 9, *C* and *D*).

Radixin and Desmosomes

Recently, it has been reported that "plakoglobin" or "band 5 protein" with a molecular mass of 83 kD, one of the major constituents of the desmosomes isolated from bovine muzzle epidermis, is also immunofluorescently localized in the adherens junction (7). When radixin was coelectrophoresed with the crude extract of the desmosomes, radixin comigrated with the unidentified minor band just beneath band 5 (plakoglobin) and above band 6 (Fig. 10, *A* and *B*) (6, 10, 22). To study the distinction between radixin and plakoglobin unequivocally, the immunological approach was used. The adherens junction extract (41) and desmosome extract (40) were electrophoresed and transferred to nitrocellulose membranes. Each membrane was divided into three strips, which were incubated with antiradixin antibody, antiplako-

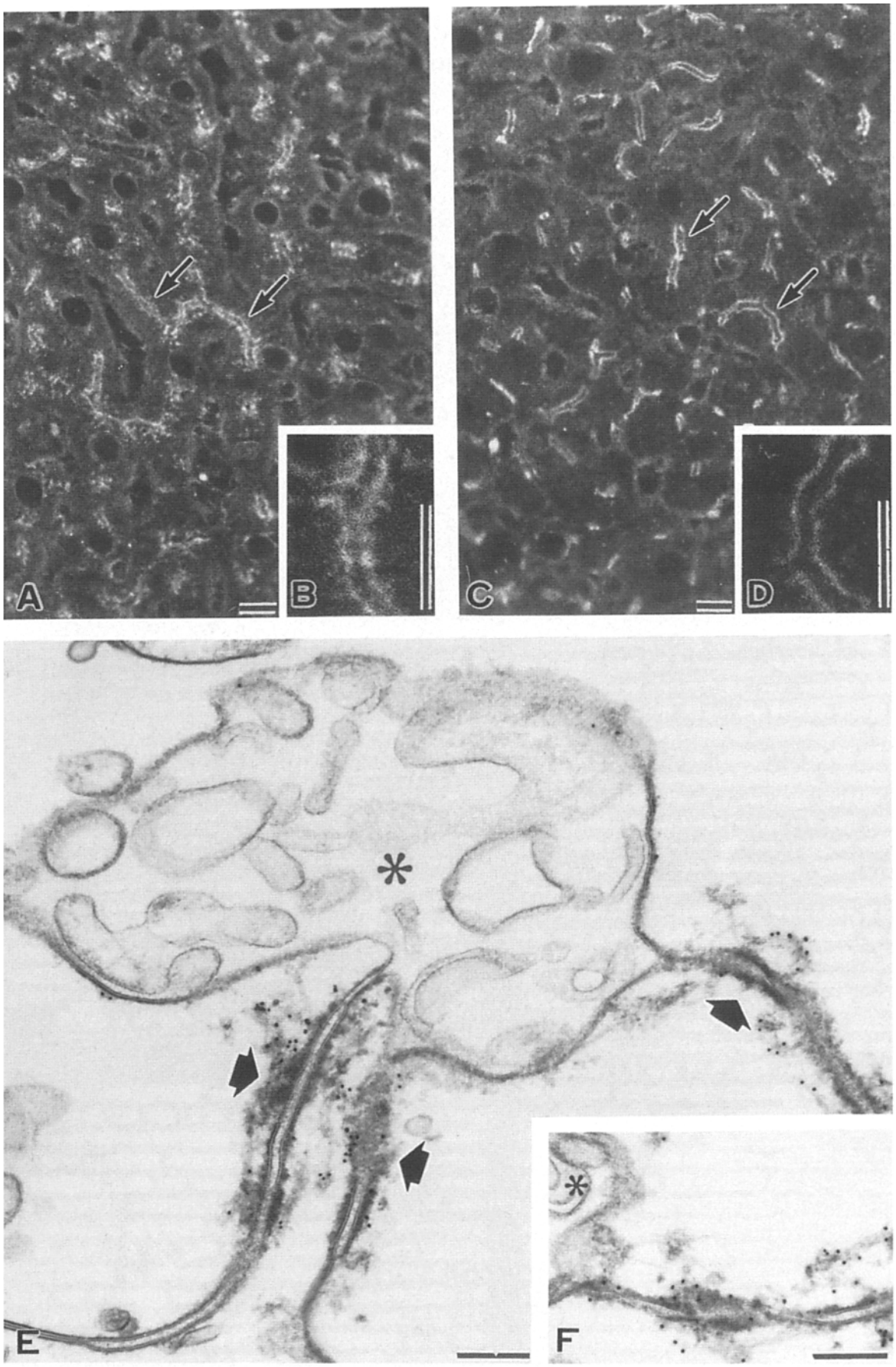
A
B
C
D
E
F

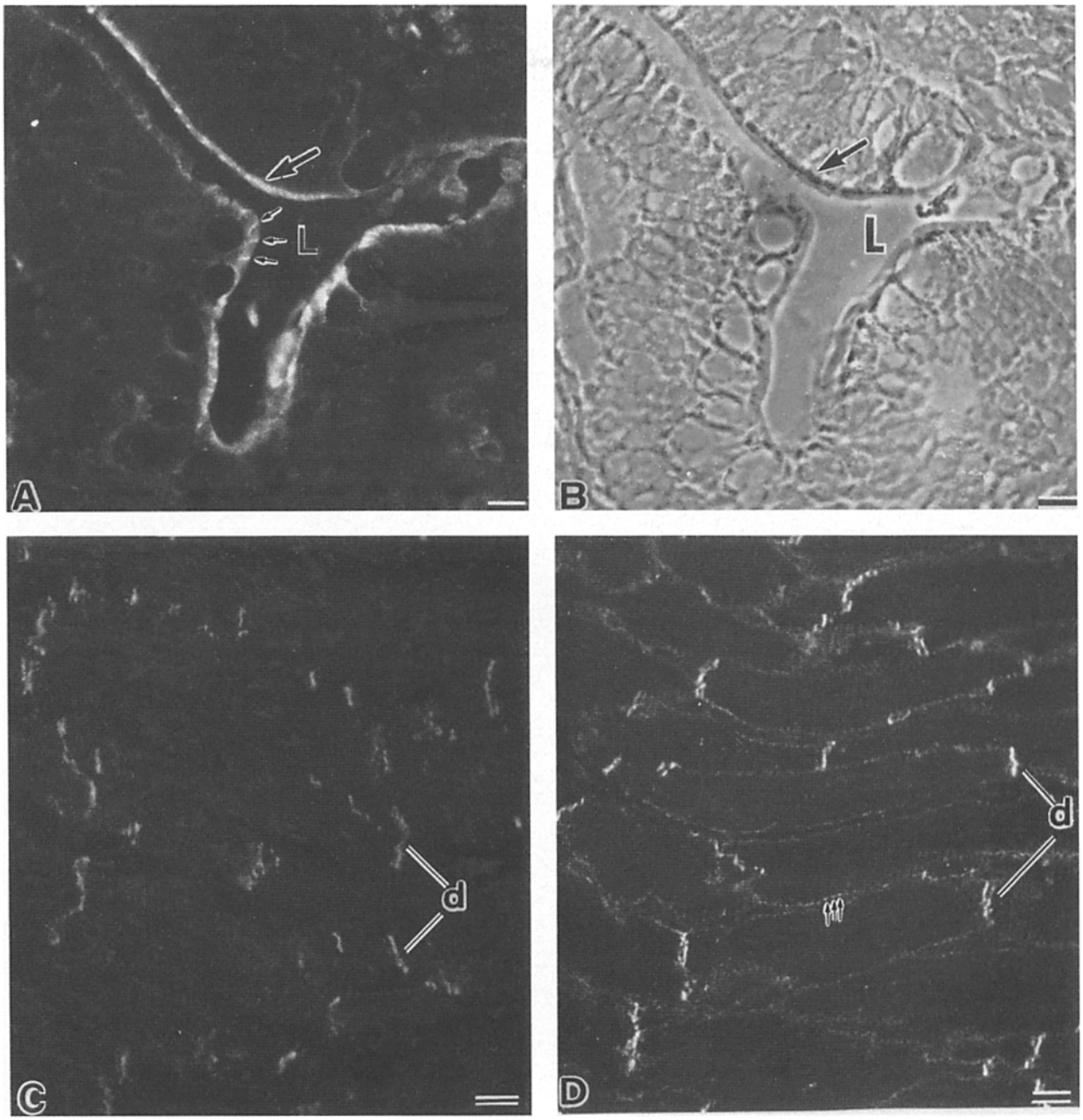

Figure 7. Localization of radixin in rat intestine (*A* and *B*) and localization of radixin (*C*) and vinculin (*D*) in rat heart. Immunofluorescence (*A*, *C*, and *D*) and phase-contrast (*B*) micrographs. Antiradixin antibodies (*A* and *B*) strongly stain the terminal web of the epithelial cells (*large arrows*) around the lumen (*L*) of the intestine. In tangential views, the radixin staining is localized in the cell-to-cell boundary (*small arrows*). Extensive staining of both antiradixin (*C*) and antivinculin (*D*) antibodies is detected in the intercalated disks (*d*). Only antivinculin represents the specific staining along the lateral side of the muscle cells in a "costamere" pattern (*arrows*). Bars, 10 μm.

Figure 6. Localization of radixin and vinculin in rat liver cells. (*A–D*) Immunofluorescence micrographs of frozen-sectioned liver cells for radixin (*A* and *B*) and vinculin (*C* and *D*). (*A* and *C*) Intense fluorescence appears on both sides of the bile canaliculi, resulting in a pair of parallel lines (*arrows*). Between *A* and *C*, the linear staining differs in appearance; i.e., it is rough and smooth, respectively, as revealed more clearly at higher magnification (*B* and *D*). Note the radixin-specific, cytoplasmic, spotted staining fairly deep within the cytoplasm (*A*). (*E* and *F*) Immunoelectron micrographs of the isolated bile canaliculi (*asterisks*)-enriched fraction with antiradixin (*E*) and antivinculin (*F*) antibodies, followed by labeling with colloidal gold-conjugated second antibodies. Radixin labeling (*E*) is associated with the undercoat of adherens junction (*arrows*), in similar distribution to vinculin staining (*F*). The distances between antigens and membranes could not be discussed in these preparations. Bars: (*A–D*) 10 μm; (*E* and *F*) 0.2 μm.

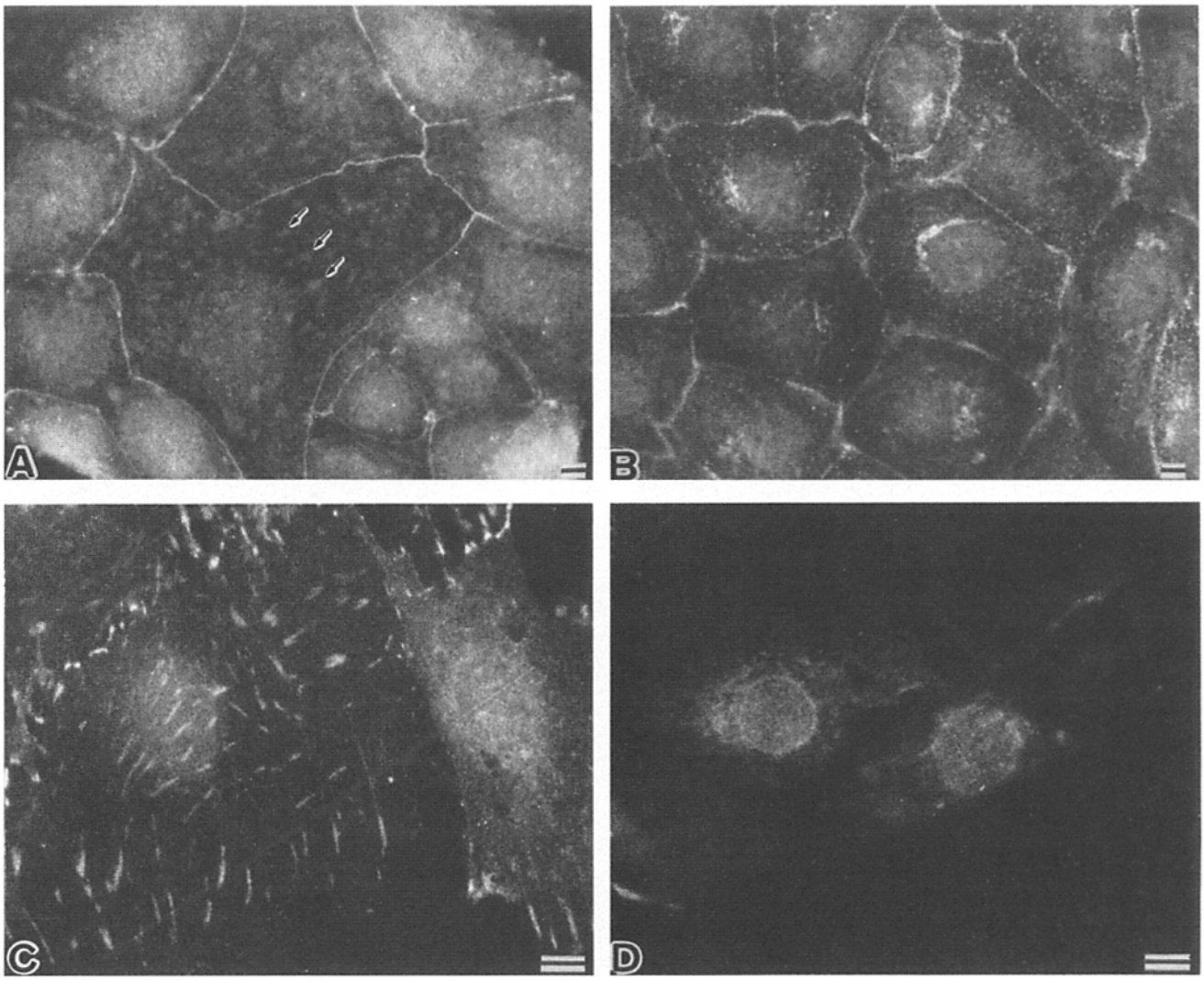

Figure 8. Immunofluorescence staining of vinculin (*A* and *C*) and radixin (*B* and *D*) in cultured cells. (*A* and *B*) MDBK cells. Both vinculin and radixin stainings were detected in the cell-to-cell adherens junction. Note that the linear stainings differ in appearance between *A* and *B*; they are smooth and rough, respectively. The cell-to-substrate adherens junctions are only stained in *A* (*arrows*), though at this focal plane they are out of focus. Radixin shows additional staining in the cytoplasm (*B*). (*C* and *D*) 3Y1 fibroblast cells. Intensive vinculin staining is detected at the cell-to-substrate adherens junctions (focal contacts) (*C*), but these junctions are by no means labeled by the antiradixin antibody (*D*). Bars, 10 μm.

globin antibody, or the mixture of these antibodies. As shown in Fig. 10, *C* and *D*, radixin and plakoglobin were recognized as distinct bands in both adherens junction extract and desmosome extract. These results have led us to conclude that radixin is distinct from plakoglobin.

The above morphological and biochemical studies have persuaded us to speculate that radixin occurs not only in adherens junctions but also in desmosomes. However, the following careful observations did not favor this speculation. As previously described (33), when the keratinocytes cultured under normal calcium conditions were doubly stained with antivinculin and antidesmoplakin antibodies, the vinculin staining on the cell-to-cell boundary was exclusive from desmoplakin staining, while these stainings were partly superimposed (Fig. 11, *A* [*a–c*] and *B*). Similar exclusive distributions were detected between radixin and desmoplakin in the cultured keratinocytes, indicating that radixin was not localized in desmosomes (Fig. 11, *C* [*a–c*] and *D*). The discrepancy between these biochemical and morphological studies remained to be studied, but the most likely explanation was that radixin in the desmosome extract might be attributed to adherens junctional or cytoplasmic radixin contaminating the desmosome fraction (17, 33).

Discussion

A new protein with a molecular mass of 82 kD has been purified from cell-to-cell adherens junctions isolated from rat liver. This purified protein appeared to act in vitro on actin in a manner similar to the so-called barbed end–capping protein. Using the polyclonal antibody specific to this protein, it has been immunologically shown that this protein is

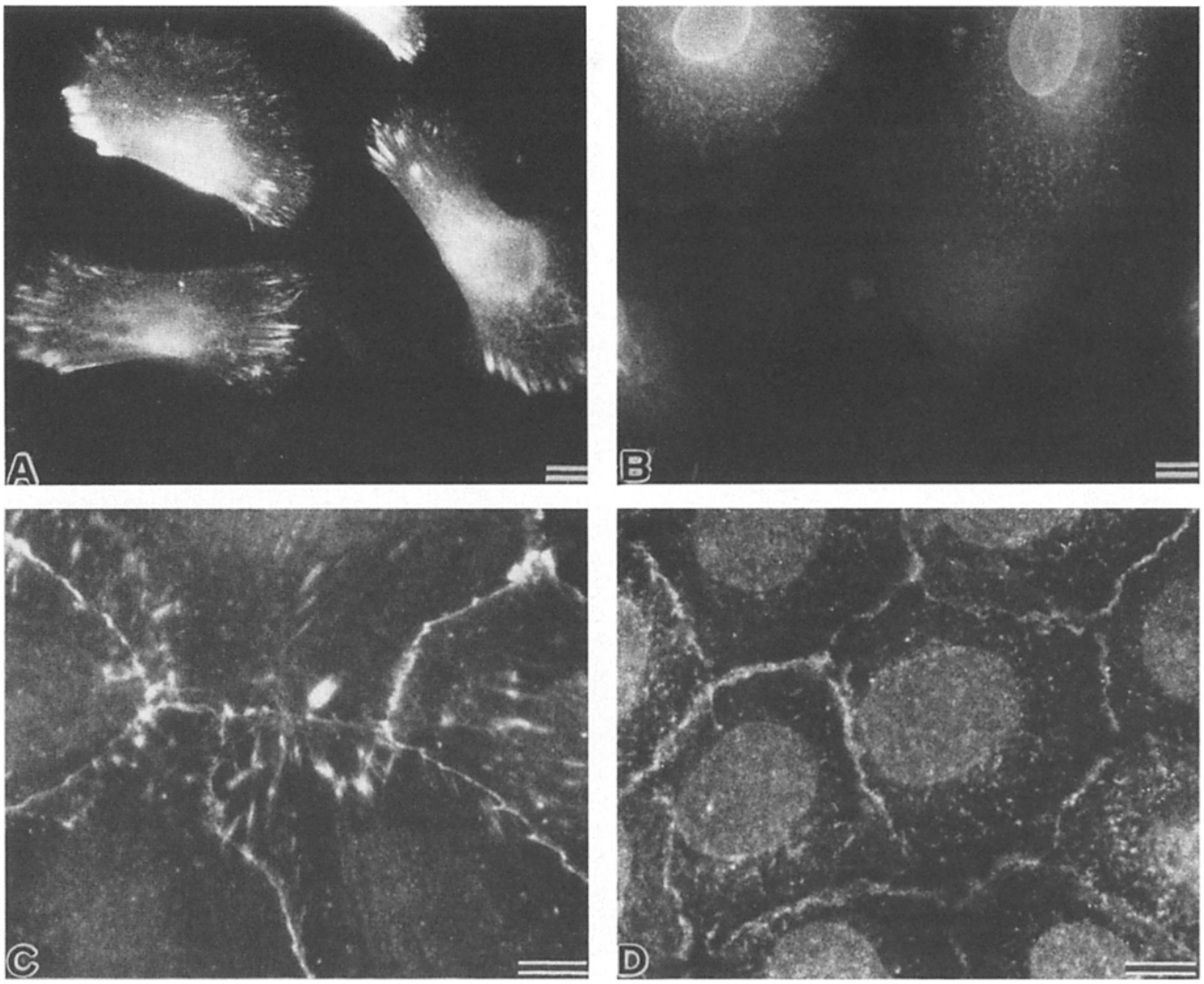

Figure 9. Localization of vinculin (*A* and *C*) and radixin (*B* and *D*) in rat keratinocytes, cultured at low (*A* and *B*) and normal (*C* and *D*) calcium concentrations. (*A* and *B*) The cell-to-substrate adherens junctions (focal contacts) are clearly stained with antivinculin antibody (*A*), but not with antiradixin antibody (*B*). (*C* and *D*) When the cell-to-cell adherens junctions are formed, vinculin is associated with both cell-to-cell and cell-to-substrate adherens junctions (*C*), whereas radixin is localized only in the cell-to-cell adherens junction (*D*). Note the radixin-specific, spotted staining in the cytoplasm in *B* and *D*. Bars, 10 μm.

localized in the undercoat of the cell-to-cell adherens junction in various types of cells. Thus, we refer to the protein as radixin.

It is now widely accepted that the undercoat of the adherens junctions play crucial roles in maintaining and organizing the actin filament bundles in nonmuscle cells. In this respect, it appears to be of great value to search for actin-modulating proteins in the undercoat of this type of junction. Actually, some actin filament cross-linking proteins, such as α-actinin (12–15, 31) and filamin (13), have been shown to localize at the undercoat. The occurrence of the barbed end–capping protein in the undercoat has been a subject of hot debate. Although vinculin was orginally reported to have a barbed end–capping activity, at present this ostensible activity is widely attributed to contaminants, and it is thought that highly purified vinculin does not cap the barbed end of actin filaments (44). Lin and colleagues (45) have intensively studied this contaminated protein mainly using immunological methods, and they recently reported that the contaminated proteins may arise from proteolysis of high molecular mass molecules. Radixin purified here is not a degradation product of this high molecular mass protein, since the antibody specific to radixin has never recognized the high molecular mass proteins in immunoblotting. The relationship between these two proteins remains to be clarified.

The studies of the capping activity of vinculin have persuaded us to consider the possibility that a minor contaminant in the radixin fraction may work as a barbed end–capping protein. However, the results obtained here do not favor this possibility. (*a*) Purified radixin was essentially free of contaminants as judged by SDS-PAGE combined with silver staining. Supposing that the barbed end–capping activity of

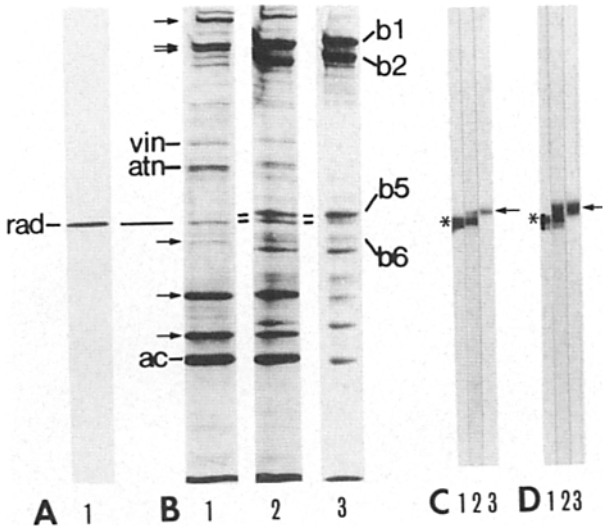

Figure 10. Coelectrophoresis of the extract of rat adherens junction with bovine desmosome extracts. Coomassie brilliant blue–stained polyacrylamide gels (*A* and *B*) and immunoblots (*C* and *D*). (*A*, lane *1*) Purified radixin (*rad*). (*B*, lane *1*) Extract of adherens junction, including vinculin (*vin*), α-actinin (*atn*), radixin (*rad*), actin (*ac*), and several other major components (*arrows*). (*B*, lane *2*) Mixture of the adherens junction and desmosome extracts. (*B*, lane *3*) The extract of isolated desmosome, including band 1 (*b1*; composed of desmoplakin I and desmocalmin), band 2 (*b2*; desmoplakin II), band 5 (*b5*; plakoglobin), and band 6 (*b6*). Radixin comigrates with the minor band just beneath band 5 and above band 6. (*C* and *D*) Immunoblots of the extract of adherens junction (*C*) or desmosomes (*D*). The nitrocellulose strips are reacted with antiradixin (*C* and *D*, lanes *1*), with the mixture of antiradixin and antiplakoglobin (*C* and *D*, lanes *2*), or with antiplakoglobin (*C* and *D*, lanes *3*). In both *C* and *D*, only band 5 (*arrows*) is specifically recognized by antiplakoglobin, and antiradixin labels a band (*asterisks*) with a molecular mass slightly smaller than band 5.

the purified radixin fraction was attributed to a minor contaminant, and that the molar ratio of this contaminant to radixin was 1:50, a very low concentration of this contaminant (contaminant/actin = 1:100,000) might reduce the final steady-state viscosity of actin solution to 60% of control viscosity (see Fig. 2 *A*). This appears to be unlikely. (*b*) Any fractions without radixin from DEAE-cellulose, DNase I–actin, and CM-cellulose columns did not effectively lower the viscosity of solutions containing actin (data not shown). (*c*) Radixin itself was trapped by the DNase I–actin column. Radixin could account for ~80% of the DNase I–binding ability of the low ionic strength extract (which included actin endogenously).

The antibody against radixin used in this study did not stain the cell-to-substrate adherens junction (focal contact) of cultured rat fibroblasts (3Y1 cells). In cultured MDBK cells and rat keratinocytes, intensive labeling was detected at the cell-to-cell adherens junctions, while there was no labeling at the cell-to-substrate junctions. Furthermore, the costamere-like staining pattern was not obtained in the cardiac muscle cells. Taken together, we can conclude that radixin was concentrated in the cell-to-cell junction, but not in the cell-to-substrate junction. Recently, by analysis of a nonimmune rabbit serum, Beckerle (1) has identified a new protein with the molecular mass of 82 kD which is localized at both cell-to-substrate and cell-to-cell adherens junctions. Since this protein was not purified and not characterized in vitro, at present it is difficult to compare it with radixin.

Another point we must discuss here is the relationship between radixin and plakoglobin. Recently, plakoglobin (with the molecular mass of 83 kD) was reported to be localized not only in desmosomes but also in the cell-to-cell adherens junctions (6, 10), though the manner of interaction between this protein and actin has not yet been clarified. The coelectrophoresis experiment has demonstrated that radixin shows slightly faster electrophoretic mobility than plakoglobin, and slower mobility than the desmosomal "band 6" protein (10, 22). The immunoblot analysis by the use of antiradixin and/or antiplakoglobin antibodies has clearly revealed that radixin and plakoglobin are distinct with each other. Furthermore, judging from the results from double immunostaining analyses, radixin is not localized in desmosomes. Taken altogether, radixin is a unique barbed end–capping protein which is specifically associated with the cell-to-cell adherens junction.

At present, it is premature to discuss the physiological functions of radixin in the cell-to-cell adherens junctions. In the previous study, we have succeeded in isolating the cell-to-cell adherens junctions from rat liver and in identifying 10 major constituents of the undercoat of the adherens junction (41). For a better understanding of the functions of radixin, our next step is to analyze the following problems. Which constituent of the undercoat or the membrane can interact with radixin? How far from the membrane is radixin localized in situ? Is radixin really associated in situ with the barbed end of actin filaments in the undercoat? And what are the chemical properties of the other constituents of the undercoat? Studies along these lines are currently being conducted in our laboratory.

We would like to express our sincere appreciation to Dr. H. Hosoya (The Tokyo Metropolitan Institue of Medical Science, Tokyo, Japan) for his helpful discussions in the actin polymerization experiments and to Dr. K. Owaribe (Nagoya University, Nagoya, Japan) for his helpful discussions in the experiments of desmosomes. We wish to thank Dr. E. Muto, Dr. S. Yonemura, Mr. T. Yagi, Mr. N. Sato, and Dr. A. Nagafuchi (The Tokyo Metropolitan Institute of Medical Science) for their valuable discussions throughout this study. We appreciate the generous gifts of the isolated acrosomal processes from Dr. I. Mabuchi (University of Tokyo, Tokyo, Japan), the antidesmoplakin antibody from Dr. A. Kusumi (University of Tokyo), and the stainless steel balls for falling ball viscometry assay from Dr. G. Matsumoto (Electrotechnical Laboratory, Ibaraki, Japan). We thank Ms. N. Funayama for her excellent assistance with photography and Ms. C. Torii for her excellent technical assistance. Our thanks are also due to Mr. Kazuto Tsukita for his encouragement.

This study was supported in part by research grants from the Ministry of Education, Science and Culture of Japan; by research grants for cardiovascular diseases from the Ministry of Health and Welfare of Japan; and by research grants from the Kazato Research Foundation.

Received for publication 3 October 1988 and in revised form 31 January 1989.

References

1. Beckerle, M. C. 1986. Identification of a new protein localized at sites of cell-substrate adhesion. *J. Cell Biol.* 103:1679–1687.

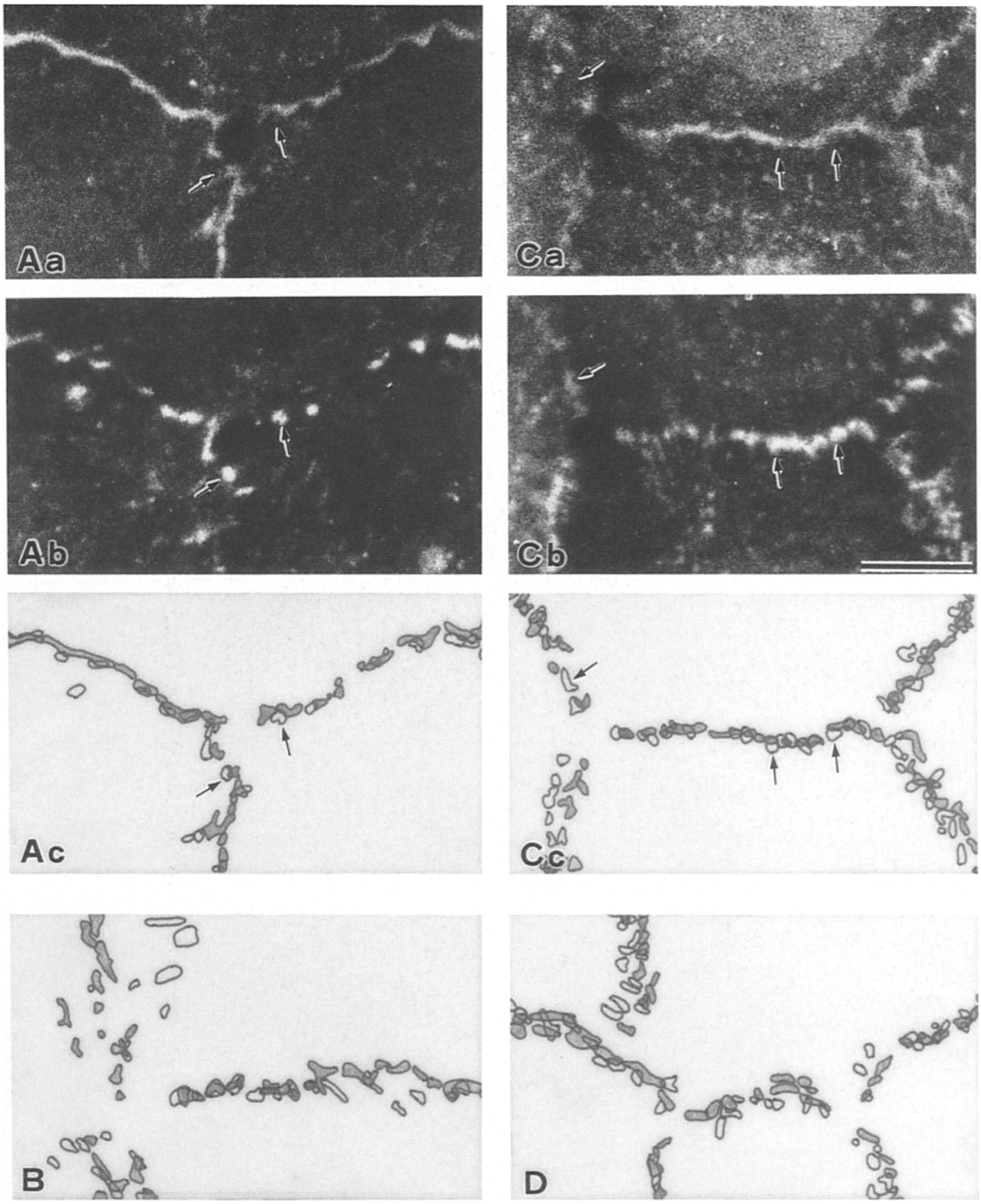

Figure 11. Comparison of the distribution of vinculin, radixin, and desmoplakin in rat keratinocytes, which are cultured at the normal calcium concentration. (*A* and *B*) Keratinocytes are doubly stained with vinculin (*Aa*) and desmoplakin (*Ab*). Their distribution areas are shown schematically in *Ac*. (*Ac*) Gray areas, vinculin; white areas, desmoplakin. Another example of the schematic drawing is shown in *B*. (*C* and *D*) Double immunofluorescence micrographs are shown for radixin (*Ca*) and desmoplakin (*Cb*) stainings. In the schematic drawing (*Cc*), radixin is localized in the gray areas and desmoplakin in the white areas. *D* is another example of the schematic drawing. Note that the desmoplakin stainings on the cell-to-cell boundaries are exclusively from vinculin staining (*arrows*, *A*) and from radixin staining (*arrows*, *C*). Bar, 10 μm.

2. Bonder, E. M., D. J. Fishkind, and M. S. Mooseker. 1983. Direct measurement of critical concentrations and assembly rate constants at the two ends of an actin filament. *Cell.* 34:491–501.
3. Bonder, E. M., and M. S. Mooseker. 1983. Direct electron microscopic visualization of barbed end capping and filament cutting by intestinal microvillar 95-kdalton protein (villin): a new actin assembly assay using the *Limulus* acrosomal process. *J. Cell Biol.* 96:1097–1107.
4. Burridge, K., and L. Connell. 1983. Talin: a cytoskeletal component concentrated in adhesion plaques and other sites of actin membrane interaction. *Cell Motil.* 3:405–417.
5. Carlsson, L., L. E. Nystrom, I. Sundkvist, F. Markey, and U. Lindberg. 1977. Actin polymerizability is influenced by profilin, a low molecular weight protein in non-muscle cells. *J. Mol. Biol.* 115:465–483.
6. Cowin, P., H.-P. Kapprell, W. W. Franke, J. Tamkun, and R. O. Hynes. 1986. Plakoglobin: a protein common to different kinds of intercellular adhering junctions. *Cell.* 46:1063–1073.
7. Craig, S. W., and T. K. Pollard. 1982. Actin-binding proteins. *Trends Biochem. Sci.* 7:88–92.
8. De Blas, A. L., and H. M. Cherwinski. 1983. Detection of antigens on nitrocellulose paper. Immunoblots with monoclonal antibody. *Anal. Biochem.* 133:214–219.
9. Farquhar, M. G., and G. E. Palade. 1963. Junctional complex in various epithelia. *J. Cell Biol.* 17:375–412.
10. Franke, W. W., H. Mueller, S. Mittnacht, H.-P. Kapprell, and J. L. Jorcano. 1983. Significance of two desmosome plaque-associated polypeptides of molecular weights 75,000 and 83,000. *EMBO (Eur. Mol. Biol. Organ.) J.* 2:2211–2215.
11. Geiger, B. 1979. A 130k protein from chicken gizzard. Its localization at the termini of microfilament bundles in cultured chicken cells. *Cell.* 18:193–205.
12. Geiger, B. 1983. Membrane-cytoskeletal interaction. *Biochem. Biophys. Acta.* 737:305–341.
13. Geiger, B., Z. Avnur, G. Rinnerthaler, H. Hinssen, and V. J. Small. 1984. Microfilament-organizing centers in areas of cell contact: cytoskeletal interactions during cell attachment and locomotion. *J. Cell Biol.* 99(suppl.): 83s–91s.
14. Geiger, B., A. H. Dutton, K. T. Tokuyasu, and S. J. Singer. 1981. Immunoelectron microscope studies of membrane–microfilament interactions. Distribution of α-actinin, tropomyosin, and vinculin in intestinal epithelial brush border and chicken gizzard smooth muscle cells. *J. Cell Biol.* 91:614–628.
15. Geiger, B., E. Schmid, and W. W. Franke. 1983. Spatial distribution of proteins specific for desmosomes and adherens junction in epithelial cells demonstrated by double immunofluorescence microscopy. *Differentiation.* 23:189–205.
16. Geiger, B., T. Volk, and T. Volberg. 1985. Molecular heterogeneity of adherens junctions. *J. Cell Biol.* 101:1523–1531.
17. Green, K. J., B. Geiger, J. C. R. Jones, J. C. Talian, and R. D. Goldman. 1987. The relationship between intermediate filaments and microfilaments before and during the formation of desmosomes and adherens-type junctions in mouse epidermal keratinocytes. *J. Cell Biol.* 104:1389–1402.
18. Hatano, S., T. Hasegawa, H. Sugino, and K. Ozaki. 1982. Physical properties of fragmin, a Ca^{2+}-sensitive regulatory protein of actin polymerization isolated from *Physarum* plasmodium. *In* Calmodulin and Intracellular Ca^{2+} Receptors. S. Kakiuchi, H. Hidaka, and A. R. Means, editors. Plenum Press, New York. 403–420.
19. Hosoya, H., and I. Mabuchi. 1984. A 45,000-mol-wt protein–actin complex from unfertilized sea urchin egg affects assembly properties of actin. *J. Cell Biol.* 99:994–1001.
20. Ishikawa, H. 1979. Identification and distribution of intracellular filaments. *In* Cell Motility: Molecules and Organization. S. Hatano, H. Ishikawa, and H. Sato, editors. University of Tokyo Press, Tokyo. 417–444.
21. Isenberg, G., K. Leonard, and B. M. Jockusch. 1982. Structural aspects of vinculin-actin interactions. *J. Mol. Biol.* 158:231–249.
22. Kapprell, H.-P., K. Owaribe, and W. W. Franke. 1988. Identification of a basic protein of M_r 75,000 as an accessory desmosomal plaque protein in stratified and complex epithelia. *J. Cell Biol.* 106:1679–1691.
23. Korn, E. D. 1982. Actin polymerization and its regulation by proteins from nonmuscle cells. *Physiol. Rev.* 62:672–737.
24. Laemmli, U. K. 1970. Cleavage of structural proteins during the assembly of the head of bacteriophage T4. *Nature (Lond.).* 227:680–685.
25. Lazarides, E., and K. Burridge. 1975. α-Actinin: immunofluorescent localization of muscle structural protein in nonmuscle cells. *Cell.* 6:289–298.
26. Mabuchi, I. 1983. Electron microscopic determination of the actin filament end at which cytochalasin B blocks monomer addition using the acrosomal actin bundle from horseshoe crab sperm. *J. Biochem. (Tokyo).* 94:1349–1352.
27. Mabuchi, I. 1983. An actin-depolymerizing protein (depactin) from starfish oocytes: properties and interaction with actin. *J. Cell Biol.* 97:1612–1621.
28. Mabuchi, I., H. Hosoya, S. Ishidate, Y. Hamaguchi, Sa. Tsukita, and Sh. Tsukita. 1985. Actin modulating proteins in echinoderm eggs II. *In* Cell Motility: Mechanism and Regulation. University of Tokyo Press, Tokyo. 175–188.
29. MacLean-Fletcher, S. D., and T. D. Pollard. 1980. Viscometric analysis of the gelation of *Acanthamoeba* extracts and purification of two gelation factors. *J. Cell Biol.* 85:414–428.
30. MacLean-Fletcher, S. D., and T. D. Pollard. 1980. Mechanism of action of cytochalasin B on actin. *Cell.* 20:329–341.
31. Maruyama, K., and S. Ebashi. 1965. α-Actinin: a new structural protein from striated muscle. II. Action on actin. *J. Biochem. (Tokyo).* 59: 422–424.
32. Nishida, E., S. Maekawa, and H. Sakai. 1984. Cofilin, a protein in porcine brain which binds to actin filaments and inhibits their interactions with myosin and tropomyosin. *Biochemistry.* 23:5307–5313.
33. O'Keefe, E., R. A. Briggaman, and B. Herman. 1987. Calcium-induced assembly of adherens junctions in keratinocytes. *J. Cell Biol.* 105:807–817.
34. Pardo, J. V., J. D. Siliciano, and S. W. Craig. 1983. A vinculin-containing cortical lattice in skeletal muscle: transverse lattice elements ("costameres") marks sites of attachment between myofibrils and sarcolemma. *Proc. Natl. Acad. Sci. USA.* 80:1008–1012.
35. Pollard, T. D., and M. S. Mooseker. 1981. Direct measurement of actin polymerization rate constants by electron microscopy of actin filaments nucleated by isolated microvillus cores. *J. Cell Biol.* 88:654–659.
36. Shriver, K., and L. Rohrschneider. 1981. Organization of $pp60^{src}$ and selected cytoskeletal protein within adhesion plaques and junction of Rous sarcoma virus–transfected rat cells. *J. Cell Biol.* 89:525–555.
37. Spudich, J. A., and S. Watt. 1971. The regulation of rabbit skeletal muscle contraction. I. Biochemical studies of the interaction of the tropomyosin–troponin complex with actin and the proteolytic fragments of myosin. *J. Biol. Chem.* 246:4866–4871.
38. Staehelin, A. 1974. Structure and function of intercellular junctions. *Int. Rev. Cytol.* 39:191–283.
39. Tilney, L. G. 1975. Actin filaments in the acrosomal reaction of *Limulus* sperm: motion generated by alterations in the packing of the filaments. *J. Cell Biol.* 64:289–310.
40. Tsukita, Sa., and Sh. Tsukita. 1985. Desmocalmin: a calmodulin-binding high molecular weight protein isolated from desmosomes. *J. Cell Biol.* 101:2070–2080.
41. Tsukita, Sh., and Sa. Tsukita. 1989. Isolation of cell-to-cell adherens junctions from rat liver. *J. Cell Biol.* 108:31–41.
42. Vaessen, R. T. M. J., J. Kreike, and G. S. P. Groot. 1981. Protein transfer to nitrocellulose filters. A simple method for quantitation of single protein in complex mixtures. *FEBS (Fed. Eur. Biochem. Soc.). Lett.* 124:193–196.
43. Weeds, A. 1982. Actin-binding proteins: regulators of cell architecture and motility. *Nature (Lond.).* 296:811–816.
44. Wilkins, J. A., and S. Lin. 1986. A re-examination of the interaction of vinculin with actin. *J. Cell Biol.* 102:1085–1092.
45. Wilkins, J. A., M. A. Risinger, and S. Lin. 1986. Studies on protein that co-purify with smooth muscle vinculin: identification of immunologically related species in focal adhesions of nonmuscle and Z-lines of muscle cells. *J. Cell Biol.* 103:1483–1494.